Depression in Premanifest Huntington's Disease: Aberrant Effective Connectivity of Striatum and Default Mode Network

Tamrin Barta[1], Leonardo Novelli[1], Nellie Georgiou-Karistianis[1], Julie Stout[1], Samantha Loi[2,3], Yifat Glikmann-Johnston[1], and Adeel Razi[1,4,5,6]

Author affiliations:

1 Turner Institute of Brain and Mental Health at the School of Psychological Sciences, and, Faculty of Medicine, Nursing and Health Sciences, Monash University

2 Department of Psychiatry, University of Melbourne.

3 Neuropsychiatry Centre, Royal Melbourne Hospital, Parkville, Australia

4 Monash Biomedical Imaging, Monash University, Clayton, Victoria, Australia

5 Wellcome Centre for Human Neuroimaging, University College London, London, United Kingdom

6 CIFAR Azrieli Global Scholars Program, CIFAR, Toronto, Ontario, Canada

Abstract

Background

Depression frequently precedes motor symptoms in Huntington's disease (HD), yet the neural mechanisms remain poorly characterized. We investigated effective connectivity between default mode network and striatal regions in premanifest HD gene expansion carriers.

Methods

We analyzed 3T resting state fMRI data from 98 premanifest participants (48.98% females; M_{age} = 42.82). Spectral dynamic causal modeling estimated subject-level connectivity, while parametric empirical Bayes determined group-level effective connectivity differences between participants with a diagnosed depression history and those without. Brain-behavior associations with clinical depression measures (HADS-D and BDI-II) were examined across current, remitted, and never-depressed states.

Results

Model estimation was excellent (89.82% variance-explained). HDGECs with depression history showed no significant MPFC-PCC connectivity alterations but exhibited decreased inhibitory PCC-to-hippocampal connectivity, increased right hippocampus-to-PCC inhibition, and greater inhibitory influence from striatum to DMN. Current versus never-depressed comparisons showed more pronounced connectivity changes, with reduced DMN influence and stronger striatum-to-DMN connections. Current versus remitted depression revealed distinct patterns with increased MPFC-to-PCC connectivity and decreased PCC-to-MPFC connectivity. Clinical measures consistently associated with altered hippocampus-PCC bidirectional connectivity across groups.

Conclusions

These findings establish distinct striatal-DMN interaction patterns in depression in premanifest HD that differ from non-neurological depression. The prominent hippocampal-DMN dysconnectivity represents emerging evidence linking these regions with depression in premanifest HD. These connectivity patterns could serve as functional biomarkers for depression in HD.

Depression is common early in Huntington's Disease (HD), in the premanifest period, up to 10 years before the onset of clinically significant motor deficits (1,2). Up to 20% of people with premanifest HD experience depression, at rates higher than the general population (3), and with significant increases in symptoms in the year prior to motor symptom onset (4). Despite the established etiology for HD as an autosomal dominant trinucleotide repeat disorder characterized by cortico-striatal degeneration (5), the pathophysiology of depression in HD patients remains poorly understood.

The etiology of depression in premanifest HD is heterogeneous and complex, involving psychosocial factors and neuropathological features (6). HD gene-expansion carriers (HDGECs) show elevated rates of depressive symptoms and major depressive disorder during the premanifest period compared to both the general population and gene-expansion negative at-risk people (1,2,7). Further, rates of depression symptoms and depressive disorders are higher for HDGECs when compared to at-risk people without the gene expansion, prior to genetic confirmation of HD status (4). This means that when accounting for shared psychosocial experiences and perception of risk, premanifest HDGECs are more likely to report elevated depression, suggesting a neuropathological underpinning. This is supported by preclinical evidence, which demonstrated depressive behaviors can be prevented through modulating huntingtin (8) and depressive behaviors associated with altered serotonergic signaling in the hippocampus and cortex in HD mouse models (9).

HD is characterized by early and severe atrophy of the striatum (5). Despite documented degeneration of the striatum in premanifest HD (10,11), there is little evidence depression is related to striatal degeneration in HD (12). The dorsal striatum—comprising caudate nucleus and putamen—is a core part of frontostriatal circuits (13), and evidence in the depression literature shows aberrant functional connectivity in depression (14), and meta-analytic evidence of volumetric reductions (15) and aberrant brain network topology (16,17) associated with this

circuitry. The makeup of frontostriatal circuitry means disruption at any point can result in dysfunction of the entire circuit, suggesting increased vulnerability to depression in HD.

Mental illnesses are posited as dysconnection syndromes, resulting from abnormal interactions between distributed brain networks (13,18,19), which has been suggested as the neuropathological basis for depression in HD (20). The default mode network (DMN) is a functional network with aberrations considered to be a reliable neural marker of depression (13,21). It comprises anterior—medial prefrontal cortex (MPFC)—and posterior hubs—posterior cingulate cortex (PCC)(22). In depression, there is demonstrated increased functional connectivity in anterior DMN, altered functional connectivity between anterior and posterior DMN (23), and increased effective connectivity from anterior to posterior DMN (24). Additionally, the hippocampus is often considered a subsystem of the DMN (23) and is associated with major depression in non-neurological populations, including hyperconnectivity between MPFC and hippocampus (25,26), and in preclinical models of HD (9). Together, aberrations in DMN connectivity could contribute to depression in premanifest HD.

Brain dysconnection between the DMN and striatum could play a substantial role in depression in premanifest HD. Notably, white matter architecture changes and grey matter volume reductions, within both the DMN and striatum, distinguishes depression in non-neurological populations (27). Depression has been linked to aberrant functional connectivity within the striatum and frontal cortex (17), between the striatum and the PCC (28), and hyperconnectivity within the DMN, including hippocampus, has extended to networks including the caudate (25). Within the HD literature, depressive symptoms in premanifest HD correlate with increased functional connectivity and decreased structural connectivity in the DMN and striatum (12), and reduced cortical thickness in the DMN and frontostriatal network across premanifest and manifest HD (29). Evidence of structural and functional changes in association with depression

in HD supports the idea that large-scale dysconnection of the striatum and DMN contribute to depression in premanifest HD.

Neuroimaging studies of depression in non-neurological populations and HD have identified differences in functional connectivity (12,21,23,25), a correlation-based measure reflecting dependencies between spatially remote regions (30,31). Functional connectivity is calculated from the blood-oxygen-level-dependent (BOLD) signal, which is comprised of neural, hemodynamic—such as cerebral blood flow (CBF)—and noise components. Ageing and neurodegenerative processes differentially impact components of the BOLD signal (32); in HD, there is demonstrated severe CBF hypoperfusion early in the disease, reduced up to half in frontotemporal and cingulate regions (33). Consequently, functional connectivity analyses may erroneously identify differences in functional MRI (fMRI) signals—due to CBF reductions—as neuronal differences (32). Effective connectivity overcomes this limitation as a model-based, biophysically informed measure that infers the directed influence of a neural system over another, disentangling contributions of neuronal and neurovascular mechanisms (34). We applied spectral dynamic causal modelling (spectral DCM), a popular method for inferring effective connectivity using resting-state fMRI data. DCM measures the direction and strength of connectivity among brain regions using Bayesian model fitting and discriminates inhibition and excitation of both bottom-up and top-down connections, allowing for inference of directed connectivity between brain regions and within region self-connectivity (i.e., synaptic activity) (34). Further, the framework allows inference of associations between changes in effective connectivity and behavioral measures (35).

We investigated whether DMN and striatal effective connectivity changes underpin depression in premanifest HD. We hypothesized increased effective connectivity from MPFC to PCC and hippocampus for participants with a history of depression compared to those without. We further hypothesized less effective connectivity from the MPFC to putamen and caudate for participants

with a history of depression compared to those without. We expected to see a positive association between current depressive symptoms and increased connectivity from anterior to posterior DMN. We hypothesized that DMN and striatal effective connectivity changes associated with increased current depression symptoms were a marker of brain connectivity that underpinned increased depressive symptoms in premanifest HDGECs.

2.0 Methods and Material

2.1 Participants

This study used data from Track-On HD, with protocol recorded in detail by Tabrizi et al., (2009) and Klöppel et al. (2015). Track-On HD was approved by local ethics committees at all participating sites—Leiden, London, Paris, and Vancouver—and participants provided written informed consent in accordance with the Declaration of Helsinki. The study included clinical and imaging data from 98 premanifest HDGECs (48 female, M_{age} = 45.66, *SD* = 9.95), after removing participants without complete data. All participants had a cytosine, adenine, guanine (CAG) repeat length greater than 39. Exclusion criteria included major psychiatric, neurological, or medical conditions, and a history of severe head injury (36). Participants were categorized into two groups based on whether they had either a remitted or current episode of diagnosed depressive disorder or no history of diagnosed depression.

2.2 Clinical Measures

Track-On HD involved a comprehensive neuropsychiatric battery, including demographic, clinical, and behavioral measures. The present study controlled for concomitant mood medication use, including antipsychotics, benzodiazepines, sodium valproate, serotonin–norepinephrine and selective serotonin reuptake inhibitors, tricyclic and tetracyclic antidepressants, and atypical medications such as hydroxyzine, lamotrigine, and mianserin. These medications were used for various reasons, including anxiety, bipolar affective disorder,

depression, irritability, panic disorder, and post-traumatic stress disorder. Even if used for reasons unrelated to mood, such as headaches, mood medication use was controlled for potential unprescribed effects on mood.

Three HD-related measures were included. The Unified Huntington's Disease Rating Scale (UHDRS) Total Motor Score (TMS) is a 15-item clinician-rated severity of motor signs with a maximum score of 124 (37). The CAG-Age Product (CAP) score model the interaction of age and CAG repeat length on disease progression ($\mathrm{CAP} = \frac{\mathrm{age} \times (\mathrm{CAG\ repeat\ length} - 30)}{6.49}$), whereby a CAP score is equal to 100 at the expected age of diagnosis (38–41). The CAP Score is not diagnostic, and HDGECs can have a score greater than 100. The Disease Burden Score (DBS) indexes the pathology impact of exposure to the abnormal huntingtin protein by modelling the impact of age and CAG repeat, and includes a constant of 35.5 (40).

2.2.1 Mood Measures

The study included two self-report measures of depressive symptoms: the Beck Depression Inventory, 2nd Edition (BDI-II) (42) and the Hospital Anxiety and Depression Scale, Depression Subscale (HADS-D) (43). The BDI-II is a 21-item self-report measure, using a 4-point Likert scale and maximum score of 63, that assesses depressive symptoms over a two-week period (42). The BDI-II has been recommended for use in HD (44) and an optimal cut-off score of 10/11 in HD discriminates clinically significant depression, with sensitivity of 1.00 and specificity of 0.66 (45). The HADS-D uses a 4-point Likert scale from 0–3, with a maximum score of 21 (43). Research in HD populations suggests an optimal cut-off of 6/7 to discriminate clinically significant depression with excellent sensitivity, 1.00, and good specificity, 0.82 (45). These cut-off scores were used to classify clinically meaningful depressive symptoms.

2.2.2 Demographic Analyses

Demographic variables were compared using Pearson's Chi-squared test or Linear Model ANOVA. For Pearson's Chi-squared tests, data used were nominal or ordinal, mutually exclusive, and groups were independent. For ANOVA, the Shapiro-Wilkins test and visual inspection of Q-Q plots and boxplots of residuals were assessed. See Supplementary Material for all plots. Some variables—i.e., BDI-II, HADS-D, UHDRS TMS, CAP Score and CAG repeat length—demonstrated non-normal distributions; this was considered acceptable as results did not impact main outcomes, i.e., spectral DCM, which does not rely on the assumption of normality of residuals.

2.3 Statistical Analyses

See Fig. 1 for an outline of the statistical pipeline, described in detail below.

2.3.1 Data Acquisition and Pre-processing

3T MRI data were acquired on two different scanner systems at four sites: Philips Achieva (Vancouver and Leiden) and Siemens TIM Trio (London and Paris). Pre-processing was performed using *fMRIPrep* v21.02.2 (46,47) and MRIQC v22.0.6 (48), using FreeSurfer v-6.0.1 (49). In brief, the pipeline included slice-timing correction, realignment, spatial normalization to Montreal Neurological Institute (MNI) space, and spatial smoothing by a 6 mm full-width half-maximum Gaussian kernel. See Supplementary Material for imaging acquisition procedures and pre-processing pipeline.

2.3.2 Selection and Extraction of Volumes of Interest

The selection of regions of interest (ROIs) and their size were based on previous research (22,50) and Neurosynth (51). Selected ROIs included the MPFC, PCC, and bilateral hippocampi, caudate, and putamen. Masks for the 8 ROIs were chosen using the WFU PickAtlas (52) for the PCC, hippocampi, caudate, and putamen, and the Stanford Willard Atlas

(53) for the MPFC. Pre-processed data underwent smoothing, and a generalized linear model (GLM) was used to regress out white matter and cerebrospinal fluid signals and 6 head motion parameters (3 translation and 3 rotational). The time series for each ROI was calculated as the first principal component of the voxels' activity within an 8 mm sphere for larger regions—MPFC and PCC—and a 6 mm sphere for all other regions. Boundaries of the masks constrained the spheres centered on MNI coordinates. Table 1 shows the ROI Montreal Neurological Institute (MNI) coordinates.

2.3.3. Dynamic Causal Modelling

Effective connectivity was estimated using spectral DCM. Spectral DCM employs a linear state-space model (explicitly separating neuronal activity and hemodynamics) to fit the cross-spectral densities of the observed BOLD signal. These data features are the frequency domain equivalent of the cross-correlation functions. Estimating a DCM in frequency domain provides computational efficiency when inverting large-scale brain networks (54).

A fully connected within-subject DCM model with no exogenous inputs (i.e., resting-state) was specified using the ROIs. After specification, the model was inverted by fitting the DCM forward model (i.e., its parameters) to provide the best prediction for the observed cross-spectral densities. For each subject, spectral DCM estimated the effective connectivity strength between each pair of ROIs and corresponding uncertainty.

The inferred effective connectivity from the first-level analysis was used for hypothesis testing of between-subjects' effects. Covariates included mood medications, sex, and the first principal component of between scanner effects (see Supplementary Material). The Parametric Empirical Bayes (PEB) framework was used to estimate the effect of a previous history of depression for each connection (35). The PEB procedure utilized within-subject connections, including both the expected strength and the covariance of connectivity parameters, and unexplained (between-

subject) noise. Lastly, Bayesian model reduction was employed as an efficient form of Bayesian model selection (35). We focused on connections with posterior probability ≥ 0.95 amounting to a strong evidence. Self-connections in DCM are modulators controlling the balance between excitation and inhibition, and are neurobiologically explained as modulating synaptic decay (34). More information about DCM self-connectivity is in the Supplementary Material.

Finally, leave-one-out cross-validation was performed for each connection that reached the significance criterion from the second-level analyses. The ability to correctly classify the left-out participant reaching the BDI-II and HADS-D clinical cut-off was assessed.

3.0 Results

3.1 General characteristics

HDGECs—grouped by a diagnosed history of depression—did not differ significantly in terms of sex, age, ethnicity, handedness, or any HD-related variables. However, premanifest HDGECs with a history of depression differed significantly from those without a history of depression in current depression diagnoses, history of suicidal ideation, use of mood medication and HADS-D scores. Participant characteristics are summarized in Table 2.

3.2 Accuracy of model estimation

The estimation of DCM models for individual participants in both groups was excellent. Average percentage variance-explained by DCM model estimation was 89.82% (*SD* = 3.89; *range* = 75.15-96.44). See Supplementary Fig. 9 for visualization of variance-explained across participants.

3.3 Effective Connectivity differences Between HDGECs with a History of Depression and Those Without

Effective connectivity of the DMN and striatum was analyzed between premanifest HDGECs with a history of depression and those without. Only connections that exceeded posterior probability ≥ .95 are reported. Fig. 2 details regional effective connectivity change between groups.

For HDGECs with a history of depression, within the DMN there was decreased inhibitory connectivity from PCC to both hippocampal regions. No connectivity changes were observed between MPFC and PCC, however, there was increased excitatory influence on right hippocampus. Right hippocampus had increased inhibitory connectivity to PCC. Within the striatum, HDGECs with a history of depression showed increased inhibitory self-connectivity of both left caudate, while the valence for right caudate self-connectivity shifted from inhibitory to excitatory for HDGECs with a history of depression. Additionally, there was increased excitatory influence of left on right caudate. Additionally, the right putamen showed decreased inhibitory connectivity to left caudate.

Between-network interactions revealed several key patterns. Striatal connectivity was notable for increased inhibitory influence on both the MPFC and PCC for HDGECs with a history of depression, including right caudate and left putamen. In terms of DMN-to-striatal connectivity, the MPFC showed decreased inhibitory connectivity to right caudate. The hippocampus showed altered connectivity patterns with striatal regions, particularly decreased inhibitory connectivity from left and right hippocampus to left caudate and increased connectivity from right hippocampus to left putamen with a shifting valence from inhibitory to excitatory for HDGECs with a history of depression. See Supplementary Table 1 for significant connections, valences and credible intervals. Leave-one-out cross-validation did not reach significance and is reported in the Supplementary materials.

3.3.2 Brain-behavior Associations

Effective connectivity of the DMN and striatum in association with meeting the clinical cut-off score for both the HADS-D and BDI-II was analyzed between premanifest HDGECs with a history of depression and those without. Only connections exceeding posterior probability ≥ .95 are reported. Fig. 3 details regional effective connectivity change between groups.

For premanifest HDGECs with a history of depression, clinical measures revealed alterations in DMN connectivity: meeting the clinical cut-off for both measures was associated with increased connectivity from right hippocampus to PCC and decreased connectivity from PCC to right hippocampus. Within the striatum, across measures, meeting the clinical cut-off was associated with decreased self-connectivity of left caudate, as well as decreased connectivity from right to left caudate. Additionally, there was increased connectivity from right putamen to left caudate. Between-network interactions showed measure-specific patterns: meeting the HADS-D clinical cut-off was associated with increased connectivity from right hippocampus to left striatum and increased connectivity from right caudate to MPFC, while meeting the BDI-II clinical cut-off showed was associated with increased connectivity from left putamen to MPFC.

For premanifest HDGECs without a history of depression, clinical measures showed distinct patterns of DMN connectivity: meeting the BDI-II clinical cut-off was associated with increased connectivity from right to left hippocampus and increased left hippocampal self-connectivity while meeting the HADS-D clinical cut-off was associated with decreased connectivity from right hippocampus to PCC. Within the striatum, clinically elevated symptoms of depression showed some consistent patterns: meeting the clinical cut-off for both measures was associated with increased right caudate self-connectivity and decreased right putamen self-connectivity. Between-network interactions showed consistent patterns: meeting the clinical cut-off for both measures was associated with decreased connectivity from right caudate to PCC, increased

connectivity from right putamen to PCC, and increased connectivity from right hippocampus to left putamen.

3.4 Current and Remitted Depression Connectivity Patterns

3.4.1 Current Versus Never Depressed Network Effective Connectivity Differences

Effective connectivity aberrations were analyzed between currently depressed HDGECs and those who had no history of depression. Fig. 4 details regional effective connectivity changes.

When comparing participants with currently diagnosed depression to those who have never been diagnosed, many connections remained significant with stronger increases and decreases in connectivity. Key differences once those without current depression were removed included the loss of influence of both hubs of the DMN, and reductions in caudate-to-caudate connectivity. Striatum to DMN connections remained influential.

3.4.2 Current Versus Remitted Depression Network Effective Connectivity Differences

Effective connectivity differences were analyzed between currently depressed HDGECs and those with remitted depression. Fig. 5 details regional effective connectivity differences.

In brief, these results showed unique connectivity aberrations for currently versus remitted depressed HDGECs, compared to nondepressed HDGECs. The MPFC had increased connectivity to PCC while PCC had decreased connectivity to MPFC, and we saw MPFC self-connectivity decrease. Some aspects remained stable, for example, putamen continued to have increased connectivity to DMN hub regions. Left hippocampus had strongly increased connectivity with striatal and DMN connections.

4.0 Discussion

Spectral DCM analysis revealed unexpected patterns of network dysfunction associated with depression in premanifest HD. Contrary to predictions, participants with depression history did not demonstrate MPFC to PCC connectivity and there was increased striatal-to-DMN connectivity. The DMN exhibited increased connectivity between hippocampal regions and PCC, while striatal connectivity displayed inhibitory patterns, except in left to right caudate connections. Clinical measures consistently demonstrated decreased caudate self-connectivity and aberrations in right hippocampus to PCC (and vice versa) connectivity, though DMN-striatum interactions varied by measure. Interestingly, when comparing current versus remitted depression, we saw DMN connectivity patterns in line with predictions with increased influence of MPFC on PCC and decreased connectivity from PCC on MPFC.

The present findings establish distinct patterns of striatal-DMN interactions associated with depressive symptoms in premanifest HD. Notably, while striatal dysfunction is a hallmark of HD (5), we found unique patterns of inhibitory and excitatory striatal connectivity between HDGECs with and without a depression history, suggesting differences may represent depression-specific alterations rather than general HD-related striatal dysfunction. This is supported by existing evidence of depression-related changes in structural and functional connectivity in HDGECs (12). Importantly, while depression history is associated with moderate alterations in striatal-DMN connectivity, current depression shows more intense connection strengths (particularly putamen-DMN connectivity), and more pronounced negative caudate connections compared to remitted states. These state-dependent differences in connection strength and directionality further support a depression-specific nature. These specific network patterns, particularly putamen-DMN connectivity and caudate inhibition, could potentially serve as functional biomarkers for depression in premanifest HD.

This is the first study, to our knowledge, to establish a link between alterations in hippocampal connectivity and depression in premanifest HD. While we found decreased inhibitory

connectivity within the DMN, particularly involving hippocampal-PCC connections, patterns were complex and direction-dependent. In keeping with existing findings in non-neurological populations, there was a propensity for right hippocampal involvement (26,55), including increased connectivity for HDGECs with depression history compared to without and decreased connectivity to PCC in association with clinically elevated symptoms of depression. Additionally, while research in non-neurological populations has shown increased right hippocampal connectivity within the ventral DMN associated with major depression (55), our findings demonstrate specific excitatory right hippocampal-putamen connections, suggesting a more complex pattern of hippocampal dysfunction than previously identified. Inhibitory PCC-hippocampal connectivity, compliments but does not replicate previous findings of increased PCC connectivity within the DMN in major depression (55). Our findings align with research in Parkinson's disease (PD), another motor disorder marked by cardinal motor symptoms, with depression rates exceeding the general population (56). Research in PD supports bidirectional aberrant connectivity between PCC and right hippocampus for premanifest HDGECs with a history of depression. These findings support hippocampal dysconnection in depression in movement disorders, and existing research in PD complements our findings of hippocampal involvement in the pathophysiology of depression in premanifest HD.

Perhaps the most striking and unexpected finding was the relatively limited influence of the MPFC in our models comparing depression history to no depression. When examining current versus remitted depression, we observed patterns of MPFC-PCC connectivity, suggesting state-dependent MPFC dysfunction. Our findings of distinct connectivity patterns between current and remitted depression can be contrasted with research examining depression treatment effects on DMN connectivity in a non-neurological population (24). Li et al. (2017) found pre-treatment depression was characterized by reduced posterior cortex coupling with other DMN regions and increased MFC-PCC coupling, with significant parietal to PCC reductions pre- to post-treatment.

Our findings showed pronounced differences between current and remitted states, particularly in MPFC connectivity and both studies support the idea that remission/treatment is associated with network changes. It is, however, possible that the limited influence of MPFC could be attributed to inconsistencies in designating specific areas within the prefrontal cortex as markers of depression. The division of the MPFC into ventral and dorsal regions is common, with no clear consensus on a precise definition or number of subdivisions (57). For instance, both the orbitofrontal and ventromedial prefrontal cortices have been implicated as core regions in depression subtypes (14). Moreover, the MPFC and ventromedial prefrontal cortex together have been linked to self-referential processes in depression (58), while models of anterior DMN have incorporated contributions from orbitofrontal, ventromedial, and dorsomedial cortices (59). It is possible that our study did not capture enough voxels to catch MPFC involvement. Though, further analyses found that excitatory influence of the MPFC on the PCC and disinhibition of the MPFC for both groups cancelled each other out at the group level (see Supplementary Material).

We found unique patterns of connectivity changes across BDI-II and HADS-D. Most clinical criteria for depression include somatic items, such as sleep and psychomotor changes, that do not discriminate well between nondepressed and depressed premanifest HDGECs, as these can be symptoms of HD unrelated to depression (6). For example, the HADS-D has better sensitivity and specificity compared to the BDI-II because it has only one somatic item (45). However, the HADS-D omits important non-somatic items, including suicidality (45). Despite this conjecture, endorsed depressive symptoms by HDGECs are largely consistent with standard diagnostic criteria (6). A combination of both measures and clinical cut-offs were used as the most clinically meaningful application for screening current depressive symptoms, given cut-offs were derived using gold-standard psychiatric interviews. Despite this, it remains possible that depression in our sample was not fully captured.

While this study demonstrates a relationship between brain network dysconnection and depression in premanifest HD, key questions remain. Firstly, the temporal pattern of depression in HD and its connection with disease progression remains contentious. Some have shown depression is unrelated to CAG repeat length (8,60,61) and disease progression (2,60,62). However, research suggests depression is linked to cognitive and motor changes rather than disease duration (63) and remains elevated for people with manifest HD compared to gene-negative people and family controls (64,65). There remains an unresolved question about effective connectivity changes in depression in HD and their association with disease stage.

This study suggests large scale network dysconnection as a neural basis for depression in premanifest HD. Aberrant effective connections were associated with self-reported history depression, which was differentially associated with coupling changes in depressive symptoms. Our findings add to our understanding of the pathophysiology of HD, and suggest defining functional brain networks of neuropsychiatric features, including depression, plays an important role in understanding the disease process.

5.0 Funding

AR and LN are funded by the Australian Research Council (DP200100757) and AR by Australian National Health and Medical Research Council Investigator Grant (Ref: 1194910). AR is affiliated with The Wellcome Centre for Human Neuroimaging supported by core funding from Wellcome [203147/Z/16/Z]. AR is a CIFAR Azrieli Global Scholar in the Brain, Mind, and Consciousness Program.

6.0 Competing interests

The authors report no competing interests.

7.0 Supplementary material

Supplementary material is available online.

8.0 Figure Legends

Figure 1 Analysis pipeline. (A) represents the pre-processing pipeline using fMRIPrep v21.02.2 and MRIQC v22.0.6. Eight regions of interest were selected, and boundaries of neuroanatomical masks constrained spheres centered on MNI coordinates. BOLD time-series were extracted from each of the eight region of interest. **(B)** represented the spectral dynamic causal modelling analysis that was fitted to BOLD time-series data. **(B1)** The DCM optimizes effective connectivity parameters to find the best explanation for the observed BOLD time-series. The DCM specified is a fully connected model of inhibitory and excitatory neural connections and the altered blood flow captured as a BOLD signal. Each participant's effective connectivity is individually estimated and is represented as an eight-by-eight matrix, where each element shows the magnitude and valence (excitatory or inhibitory) between a pair of regions of interest. **(B2)** The Parametric Empirical Bayes (PEB) framework was used to estimate group means and the effect of a previous history of depression for each connection. The PEB procedure, a random effects model, utilizes the first level full posteriors (mean and covariance of each connection), covariates (sex, medication, between scanner effects) and between subject noise. Bayesian model reduction is then applied to find the most parsimonious model at the group level. **(C)** Leave-one-out cross-validation was applied, a single participant that is left out in a set, highlighted in purple.

Figure 2 Difference in Mean Effective Connectivity Between Premanifest HD People with a History of Depression Versus Without. (L) Left panel shows the connectivity matrix for depression history, with increased connectivity in yellow-red and decreased connectivity in aqua-navy. **(R)** Effective connections that reached significance are shown in the dorsal plane. Nodes in purple represent the bilateral caudate and putamen (striatum), while those in green represent the medial prefrontal cortex, posterior cingulate cortex, and bilateral hippocampi (default mode network). The arrows show the directed influence of one region on another, including self-connections. Solid lines represent increased connectivity while dashes represent decreased connectivity. MPFC = Medial Prefrontal Cortex; PCC = Posterior Cingulate Cortex; HPC_L = Left Hippocampus; HPC_R = Right Hippocampus; CAU_L = Left Caudate; CAU_R = Left Caudate; PU_L = Left Putamen; PU_R = Right Putamen.

Figure 3 Effective Connectivity of DMN And Striatum in Association with Meeting Clinical Cut-Off for HADS-D And BDI-II. (A1) Regional connectivity changes for HDGECs with depression history associated with meeting clinical cut-off for BDI-II. **(A2)** Regional connectivity changes for HDGECs with depression history associated with meeting clinical cut-off for HADS-D. **(A3)** Regional connectivity changes for HDGECs with no depression history associated

with meeting clinical cut-off for BDI-II. **(A4)** Regional connectivity changes for HDGECs with no depression history associated with meeting clinical cut-off for HADS-D. The arrows show the directed influence of one region on another, including self-connections. Solid lines represent increased connectivity while dashes represent decreased connectivity. MPFC = Medial Prefrontal Cortex; PCC = Posterior Cingulate Cortex; HPC_L = Left Hippocampus; HPC_R = Right Hippocampus; CAU_L = Left Caudate; CAU_R = Left Caudate; PU_L = Left Putamen; PU_R = Right Putamen.

Figure 4 Difference in Mean Effective Connectivity Between Premanifest HD People with Current Depression versus no Depression History. (L) Left panel shows the connectivity matrix for current depression (with no depression as the reference), with increased connectivity in yellow-red and decreased connectivity in aqua-navy. **(R)** Effective connections that reached significance are shown in the dorsal plane. Nodes in purple represent the bilateral caudate and putamen (striatum), while those in green represent the medial prefrontal cortex, posterior cingulate cortex, and bilateral hippocampi (default mode network). The arrows show the directed influence of one region on another, including self-connections. Solid lines represent increased connectivity while dashes represent decreased connectivity. MPFC = Medial Prefrontal Cortex; PCC = Posterior Cingulate Cortex; HPC_L = Left Hippocampus; HPC_R = Right Hippocampus; CAU_L = Left Caudate; CAU_R = Left Caudate; PU_L = Left Putamen; PU_R = Right Putamen

Figure 5 Difference in Mean Effective Connectivity Between Premanifest HD People with Current Depression versus Remitted Depression. (L) Left panel shows the connectivity matrix for matrix for current depression (with remitted depression as the reference), with increased connectivity in yellow-red and decreased connectivity in aqua-navy. **(R)** Effective connections that reached significance are shown in the dorsal plane. Nodes in purple represent the bilateral caudate and putamen (striatum), while those in green represent the medial prefrontal cortex, posterior cingulate cortex, and bilateral hippocampi (default mode network). The arrows show the directed influence of one region on another, including self-connections. Solid lines represent increased connectivity while dashes represent decreased connectivity. MPFC = Medial Prefrontal Cortex; PCC = Posterior Cingulate Cortex; HPC_L = Left Hippocampus; HPC_R = Right Hippocampus; CAU_L = Left Caudate; CAU_R = Left Caudate; PU_L = Left Putamen; PU_R = Right Putamen

9.0 References

1. Duff K, Paulsen JS, Beglinger LJ, Langbehn DR, Stout JC. Psychiatric Symptoms in Huntington's Disease before Diagnosis: The Predict-HD Study. Biol Psychiatry. 2007 Dec 15;62(12):1341–6.

2. Kingma EM, van Duijn E, Timman R, van der Mast RC, Roos RAC. Behavioural problems in Huntington's disease using the Problem Behaviours Assessment. Gen Hosp Psychiatry. 2008 Mar 1;30(2):155–61.

3. Paulsen JS, Nehl C, Hoth KF, Kanz JE, Benjamin M, Conybeare R, et al. Depression and Stages of Huntington's Disease. J Neuropsychiatry Clin Neurosci. 2005 Nov;17(4):496–502.

4. Julien CL, Thompson JC, Wild S, Yardumian P, Snowden JS, Turner G, et al. Psychiatric disorders in preclinical Huntington's disease. J Neurol Neurosurg Psychiatry. 2007 Sep;78(9):939–43.

5. Ross CA, Tabrizi SJ. Huntington's disease: from molecular pathogenesis to clinical treatment. Lancet Neurol. 2011 Jan 1;10(1):83–98.

6. Bilal H, Warren N, Dahanayake P, Kelso W, Farrand S, Stout JC. The Lived Experiences of Depression in Huntington's Disease: A Qualitative Study. J Huntingt Dis. 2022 Jan 1;11(3):321–35.

7. van Duijn E, Kingma EM, Timman R, Zitman FG, Tibben A, Roos RAC, et al. Cross-Sectional Study on Prevalences of Psychiatric Disorders in Mutation Carriers of Huntington's Disease Compared With Mutation-Negative First-Degree Relatives. J Clin Psychiatry. 2008 Nov 30;69(11):3949.

8. Pouladi MA, Graham RK, Karasinska JM, Xie Y, Santos RD, Petersén Å, et al. Prevention of depressive behaviour in the YAC128 mouse model of Huntington disease by mutation at residue 586 of huntingtin. Brain. 2009 Apr 1;132(4):919–32.

9. Pang TYC, Du X, Zajac MS, Howard ML, Hannan AJ. Altered serotonin receptor expression is associated with depression-related behavior in the R6/1 transgenic mouse model of Huntington's disease. Hum Mol Genet. 2009 Feb 15;18(4):753–66.

10. Georgiou-Karistianis N, Gray MA, Domínguez D JF, Dymowski AR, Bohanna I, Johnston LA, et al. Automated differentiation of pre-diagnosis Huntington's disease from healthy control individuals based on quadratic discriminant analysis of the basal ganglia: The IMAGE-HD study. Neurobiol Dis. 2013 Mar 1;51:82–92.

11. Tabrizi SJ, Langbehn DR, Leavitt BR, Roos RA, Durr A, Craufurd D, et al. Biological and clinical manifestations of Huntington's disease in the longitudinal TRACK-HD study: cross-sectional analysis of baseline data. Lancet Neurol. 2009 Sep 1;8(9):791–801.

12. McColgan P, Razi A, Gregory S, Seunarine KK, Durr A, A.C. Roos R, et al. Structural and functional brain network correlates of depressive symptoms in premanifest Huntington's disease. Hum Brain Mapp. 2017;38(6):2819–29.

13. Li B, Friston K, Mody M, Wang HN, Lu HB, Hu DW. A brain network model for depression: From symptom understanding to disease intervention. CNS Neurosci Ther. 2018;24(11):1004–19.

14. Drysdale AT, Grosenick L, Downar J, Dunlop K, Mansouri F, Meng Y, et al. Resting-state connectivity biomarkers define neurophysiological subtypes of depression. Nat Med. 2017 Jan;23(1):28–38.

15. Bora E, Harrison BJ, Davey CG, Yücel M, Pantelis C. Meta-analysis of volumetric abnormalities in cortico-striatal-pallidal-thalamic circuits in major depressive disorder. Psychol Med. 2012 Apr;42(4):671–81.

16. Lynch CJ, Elbau IG, Ng T, Ayaz A, Zhu S, Wolk D, et al. Frontostriatal salience network expansion in individuals in depression. Nature. 2024 Sep 4;1–10.

17. Meng C, Brandl F, Tahmasian M, Shao J, Manoliu A, Scherr M, et al. Aberrant topology of striatum's connectivity is associated with the number of episodes in depression. Brain. 2014 Feb 1;137(2):598–609.

18. Friston KJ. The disconnection hypothesis. Schizophr Res. 1998 Mar 10;30(2):115–25.

19. Friston KJ, Frith CD. Schizophrenia: a disconnection syndrome? Clin Neurosci N Y N. 1995;3(2):89–97.

20. Hannan AJ. Synaptopathy, circuitopathy and the computational biology of Huntington's disease. BMC Biol. 2018 Jun 27;16(1):71.

21. Li B, Liu L, Friston KJ, Shen H, Wang L, Zeng LL, et al. A Treatment-Resistant Default Mode Subnetwork in Major Depression. Biol Psychiatry. 2013 Jul 1;74(1):48–54.

22. Di X, Biswal BB. Identifying the default mode network structure using dynamic causal modeling on resting-state functional magnetic resonance imaging. NeuroImage. 2014 Feb 1;86:53–9.

23. Mulders PC, van Eijndhoven PF, Schene AH, Beckmann CF, Tendolkar I. Resting-state functional connectivity in major depressive disorder: A review. Neurosci Biobehav Rev. 2015 Sep 1;56:330–44.

24. Li L, Li B, Bai Y, Liu W, Wang H, Leung HC, et al. Abnormal resting state effective connectivity within the default mode network in major depressive disorder: A spectral dynamic causal modeling study. Brain Behav. 2017;7(7):e00732.

25. Kaiser RH, Andrews-Hanna JR, Wager TD, Pizzagalli DA. Large-scale network dysfunction in Major Depressive Disorder: Meta-analysis of resting-state functional connectivity. JAMA Psychiatry. 2015 Jun 1;72(6):603–11.

26. Wang Z, Yuan Y, Bai F, Shu H, You J, Li L, et al. Altered functional connectivity networks of hippocampal subregions in remitted late-onset depression: a longitudinal resting-state study. Neurosci Bull. 2015 Feb 1;31(1):13–21.

27. Grieve SM, Korgaonkar MS, Koslow SH, Gordon E, Williams LM. Widespread reductions in gray matter volume in depression. NeuroImage Clin. 2013 Jan 1;3:332–9.

28. Furman DJ, Hamilton JP, Gotlib IH. Frontostriatal functional connectivity in major depressive disorder. Biol Mood Anxiety Disord. 2011 Dec 8;1:11.

29. Garcia-Gorro C, Llera A, Martinez-Horta S, Perez-Perez J, Kulisevsky J, Rodriguez-Dechicha N, et al. Specific patterns of brain alterations underlie distinct clinical profiles in Huntington's disease. NeuroImage Clin. 2019 Jan 1;23:101900.

30. Friston KJ. Functional and Effective Connectivity: A Review. Brain Connect. 2011 Jan;1(1):13–36.

31. Friston KJ, Kahan J, Biswal B, Razi A. A DCM for resting state fMRI. NeuroImage. 2014 Jul 1;94:396–407.

32. Tsvetanov KA, Henson RNA, Rowe JB. Separating vascular and neuronal effects of age on fMRI BOLD signals. Philos Trans R Soc B Biol Sci. 2021 Jan 4;376(1815):20190631.

33. Chen JJ, Salat DH, Rosas HD. Complex Relationships between Cerebral Blood Flow and Brain Atrophy in Early Huntington's Disease. NeuroImage. 2012 Jan 16;59(2):1043–51.

34. Friston KJ, Harrison L, Penny W. Dynamic causal modelling. NeuroImage. 2003 Aug 1;19(4):1273–302.

35. Friston KJ, Litvak V, Oswal A, Razi A, Stephan KE, van Wijk BCM, et al. Bayesian model reduction and empirical Bayes for group (DCM) studies. NeuroImage. 2016 Mar 1;128:413–31.

36. Klöppel S, Gregory S, Scheller E, Minkova L, Razi A, Durr A, et al. Compensation in Preclinical Huntington's Disease: Evidence From the Track-On HD Study. EBioMedicine. 2015 Oct 1;2(10):1420–9.

37. Huntington Study Group (Kieburtz K, primary author). The Unified Huntington's Disease Rating Scale: Reliability and Consistency. Mov Disord. 1996;11(2):136–42.

38. Warner JH, Long JD, Mills JA, Langbehn DR, Ware J, Mohan A, et al. Standardizing the CAP Score in Huntington's Disease by Predicting Age-at-Onset. J Huntingt Dis. 2022;11(2):153–71.

39. Langbehn DR, Hayden MR, Paulsen JS, and the PREDICT-HD Investigators of the Huntington Study Group. CAG-repeat length and the age of onset in Huntington disease (HD): a review and validation study of statistical approaches. Am J Med Genet Part B Neuropsychiatr Genet Off Publ Int Soc Psychiatr Genet. 2010 Mar 5;153B(2):397–408.

40. Penney JB, Vonsattel JP, MacDonald ME, Gusella JF, Myers RH. CAG repeat number governs the development rate of pathology in Huntington's disease. Ann Neurol. 1997;41(5):689–92.

41. Zhang Y, Long JD, Mills JA, Warner JH, Lu W, Paulsen JS, et al. Indexing disease progression at study entry with individuals at-risk for Huntington disease. Am J Med Genet B Neuropsychiatr Genet. 2011;156(7):751–63.

42. Beck AT, Steer RA, Brown GK, others. Manual for the Beck depression inventory-II. San Antonio TX Psychol Corp. 1996;1(82):10–1037.

43. Zigmond AS, Snaith RP. The hospital anxiety and depression scale. Acta Psychiatr Scand. 1983;67(6):361–70.

44. Mestre TA, van Duijn E, Davis AM, Bachoud-Lévi AC, Busse M, Anderson KE, et al. Rating scales for behavioral symptoms in Huntington's disease: Critique and recommendations. Mov Disord. 2016;31(10):1466–78.

45. De Souza J, Jones LA, Rickards H. Validation of self-report depression rating scales in Huntington's disease. Mov Disord. 2010;25(1):91–6.

46. Esteban O, Markiewicz CJ, Blair RW, Moodie CA, Isik AI, Erramuzpe A, et al. fMRIPrep: a robust preprocessing pipeline for functional MRI. Nat Methods. 2019 Jan;16(1):111–6.

47. Esteban O, Ciric R, Finc K, Blair RW, Markiewicz CJ, Moodie CA, et al. Analysis of task-based functional MRI data preprocessed with fMRIPrep. Nat Protoc. 2020 Jul;15(7):2186–202.

48. Esteban O, Birman D, Schaer M, Koyejo OO, Poldrack RA, Gorgolewski KJ. MRIQC: Advancing the automatic prediction of image quality in MRI from unseen sites. PLOS ONE. 2017 Sep 25;12(9):e0184661.

49. Reuter M, Schmansky NJ, Rosas HD, Fischl B. Within-subject template estimation for unbiased longitudinal image analysis. Neuroimage. 2012 Jul 16;61(4):1402–18.

50. Razi A, Kahan J, Rees G, Friston KJ. Construct validation of a DCM for resting state fMRI. NeuroImage. 2015 Feb 1;106:1–14.

51. Yarkoni T, Poldrack RA, Nichols TE, Van Essen DC, Wager TD. Large-scale automated synthesis of human functional neuroimaging data. Nat Methods. 2011 Jun 26;8(8):665–70.

52. Maldjian J, Laurienti P, Kraft R, Burdette J. An automated method for neuroanatomic and cytoarchitectonic atlas-based interrogation of fMRI data sets. Neuroimage. 2003 Jul 25;

53. Altmann A, Ng B, Landau SM, Jagust WJ, Greicius MD. Regional brain hypometabolism is unrelated to regional amyloid plaque burden. Brain. 2015 Dec;138(12):3734–46.

54. Novelli L, Friston K, Razi A. Spectral dynamic causal modeling: A didactic introduction and its relationship with functional connectivity. Netw Neurosci. 2024 Jan 19;1–25.

55. Sambataro F, Wolf ND, Pennuto M, Vasic N, Wolf RC. Revisiting default mode network function in major depression: evidence for disrupted subsystem connectivity. Psychol Med. 2014 Jul;44(10):2041–51.

56. Lim J, Bang Y, Choi HJ. Abnormal hippocampal neurogenesis in Parkinson's disease: relevance to a new therapeutic target for depression with Parkinson's disease. Arch Pharm Res. 2018 Oct;41(10):943–54.

57. Lemogne C, Delaveau P, Freton M, Guionnet S, Fossati P. Medial prefrontal cortex and the self in major depression. J Affect Disord. 2012 Jan 1;136(1):e1–11.

58. Sheline YI, Barch DM, Price JL, Rundle MM, Vaishnavi SN, Snyder AZ, et al. The default mode network and self-referential processes in depression. Proc Natl Acad Sci. 2009 Feb 10;106(6):1942–7.

59. Zhu X, Wang X, Xiao J, Liao J, Zhong M, Wang W, et al. Evidence of a Dissociation Pattern in Resting-State Default Mode Network Connectivity in First-Episode, Treatment-Naive Major Depression Patients. Biol Psychiatry. 2012 Apr 1;71(7):611–7.

60. Berrios GE, Wagle AC, Marková IS, Wagle SA, Ho LW, Rubinsztein DC, et al. Psychiatric symptoms and CAG repeats in neurologically asymptomatic Huntington's disease gene carriers. Psychiatry Res. 2001 Jul 24;102(3):217–25.

61. Craufurd D, Thompson JC, Snowden JS. Behavioral changes in Huntington Disease. Neuropsychiatry Neuropsychol Behav Neurol. 2001 Dec;14(4):219–26.

62. Reedeker W, van der Mast RC, Giltay EJ, Kooistra TAD, Roos RAC, van Duijn E. Psychiatric Disorders in Huntington's Disease: A 2-Year Follow-up Study. Psychosomatics. 2012 May 1;53(3):220–9.

63. Dale M, Maltby J, Shimozaki S, Cramp R, Rickards H. Disease stage, but not sex, predicts depression and psychological distress in Huntington's disease: A European population study. J Psychosom Res. 2016 Jan 1;80:17–22.

64. Connors MH, Teixeira-Pinto A, Loy CT. Apathy and Depression in Huntington's Disease: Distinct Longitudinal Trajectories and Clinical Correlates. J Neuropsychiatry Clin Neurosci. 2022 Sep 21;appi.neuropsych.21070191.

65. Maltby J, Ovaska-Stafford N, Gunn S. The structure of mental health symptoms in Huntington's disease: Comparisons with healthy populations. J Clin Exp Neuropsychol. 2021 Aug 9;43(7):737–52.

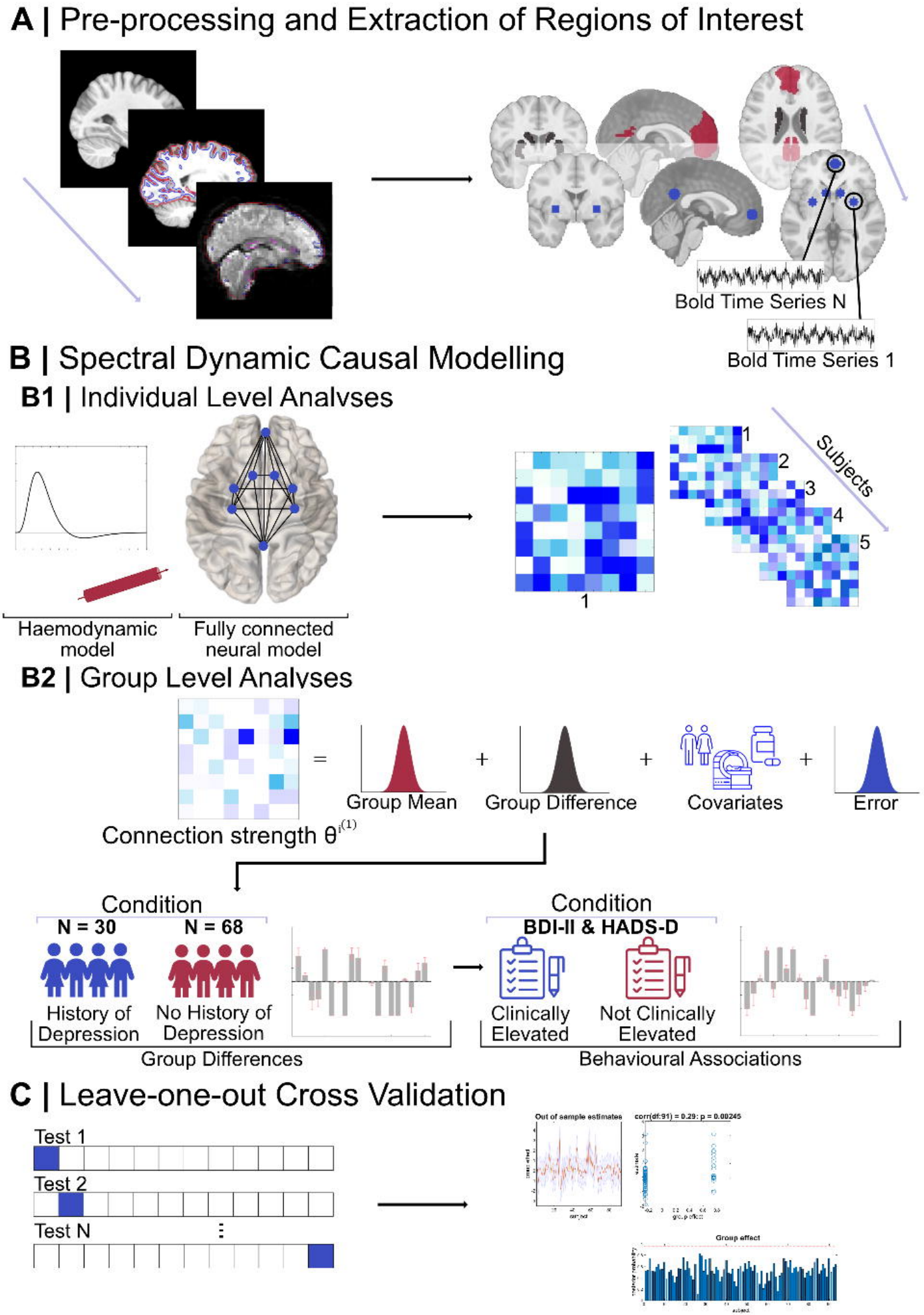
A | Pre-processing and Extraction of Regions of Interest
Bold Time Series N
Bold Time Series 1
B | Spectral Dynamic Causal Modelling
B1 | Individual Level Analyses
Haemodynamic model
Fully connected neural model
Subjects
1
2
3
4
5
B2 | Group Level Analyses
Connection strength θ(1)
Group Mean
Group Difference
Covariates
Error
Condition
N = 30
N = 68
History of Depression
No History of Depression
Group Differences
Condition
BDI-II & HADS-D
Clinically Elevated
Not Clinically Elevated
Behavioural Associations
C | Leave-one-out Cross Validation
Test 1
Test 2
Test N
Out of sample estimates
corr(df:91) = 0.29; p = 0.00245
Group effect

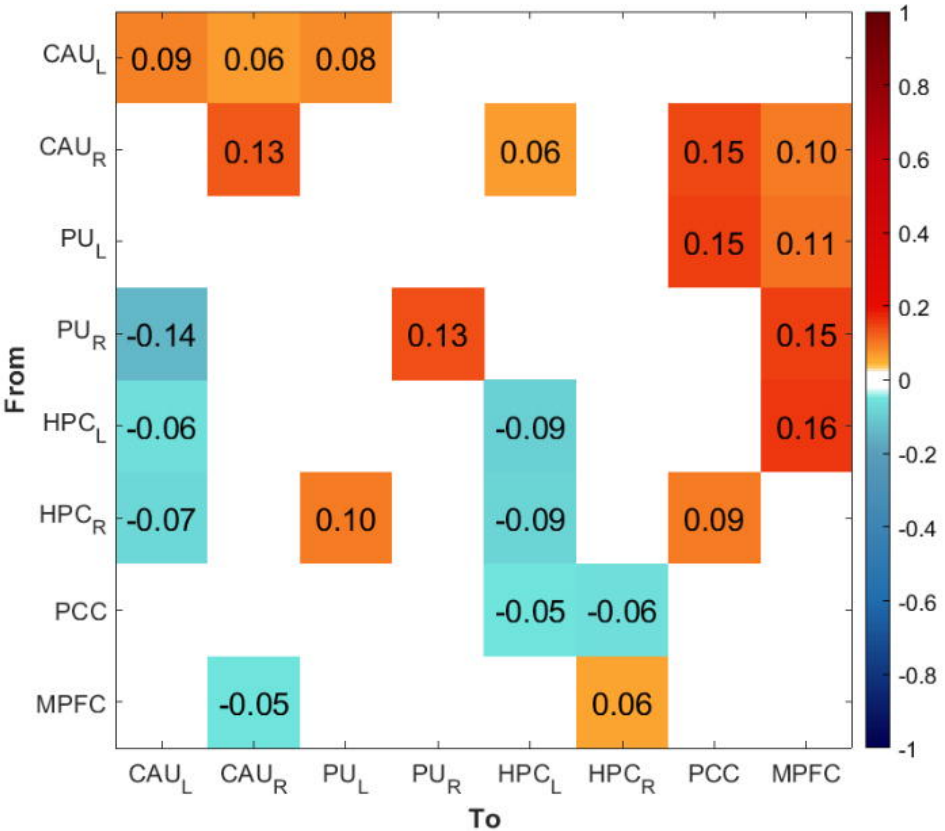
From
To
CAU_L
CAU_R
PU_L
PU_R
HPC_L
HPC_R
PCC
MPFC
0.09 0.06 0.08
0.13 0.06 0.15 0.10
0.15 0.11
-0.14 0.13 0.15
-0.06 -0.09 0.16
-0.07 0.10 -0.09 0.09
-0.05 -0.06
-0.05 0.06
1
0.8
0.6
0.4
0.2
0
-0.2
-0.4
-0.6
-0.8
-1

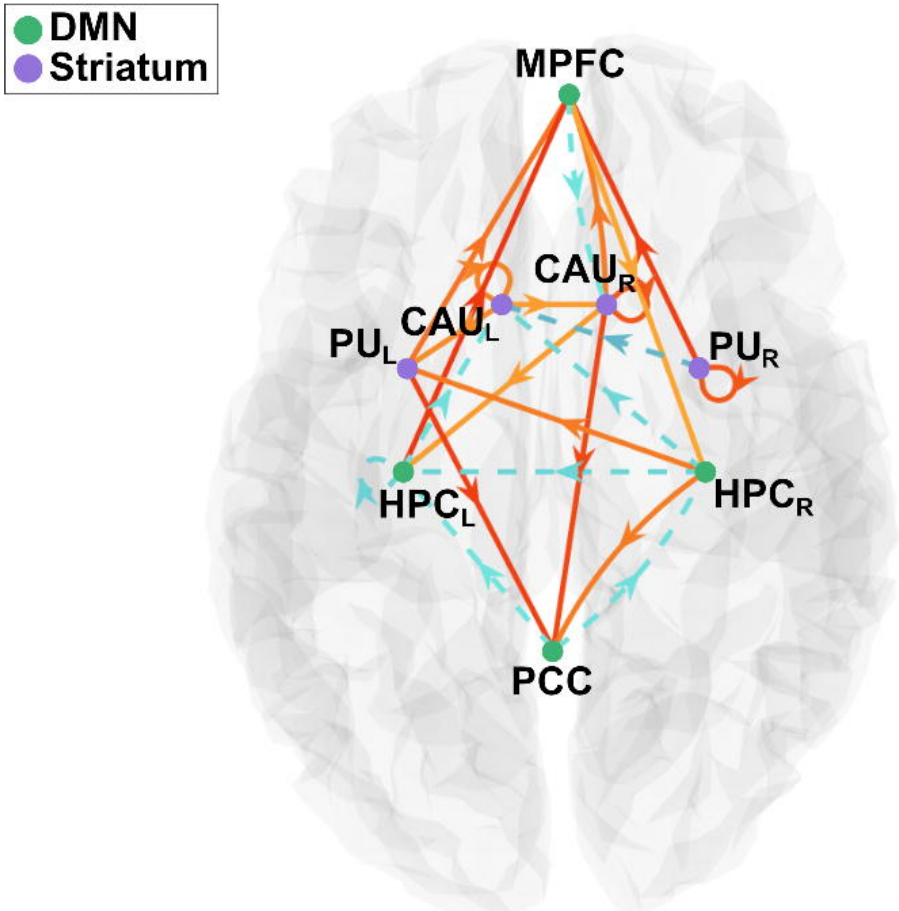
DMN
Striatum
MPFC
CAU_R
CAU_L
PU_L
PU_R
HPC_L
HPC_R
PCC

A1 | BDI-II Scores for HDGECs with a history of depression

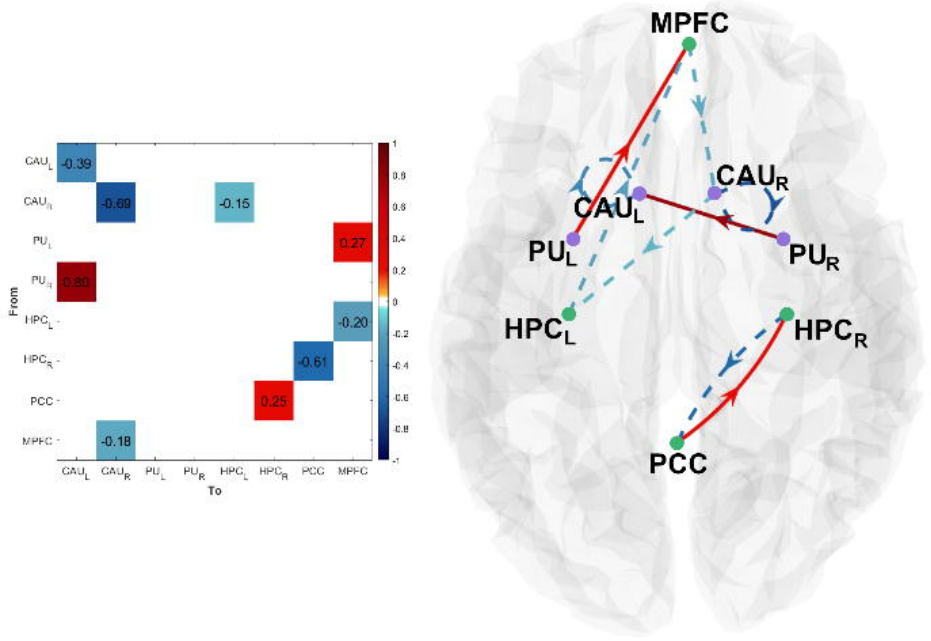

A2 | HADS-D Scores for HDGECs with a history of depression

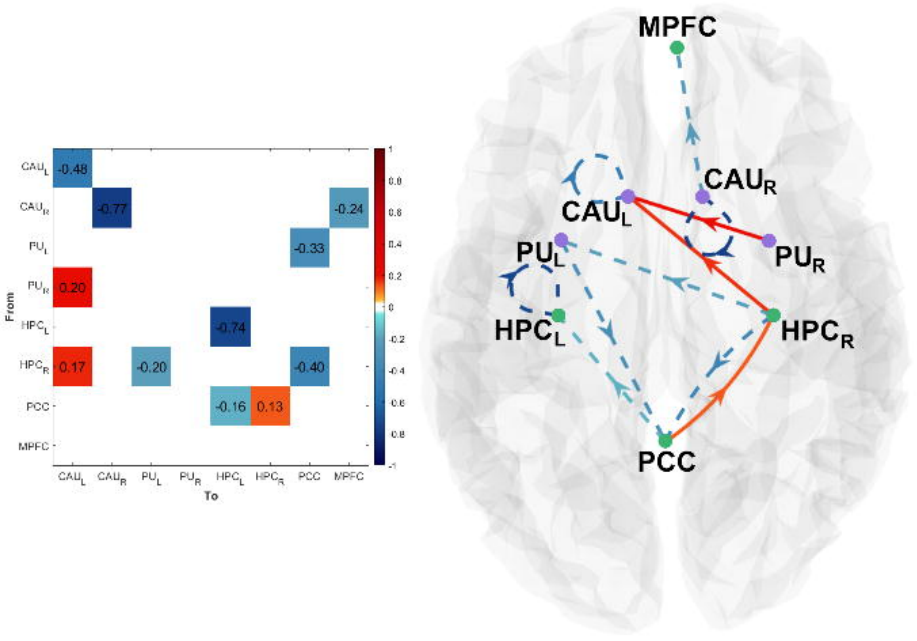

B1 | BDI-II Scores for HDGECs with no history of depression

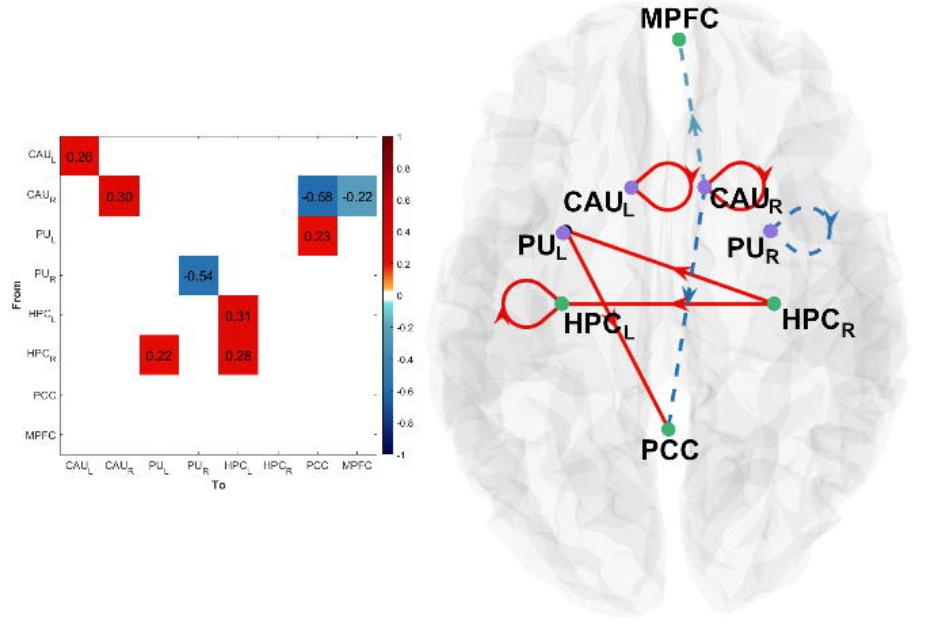

B2 | HADS-D Scores for HDGECs with no history of depression

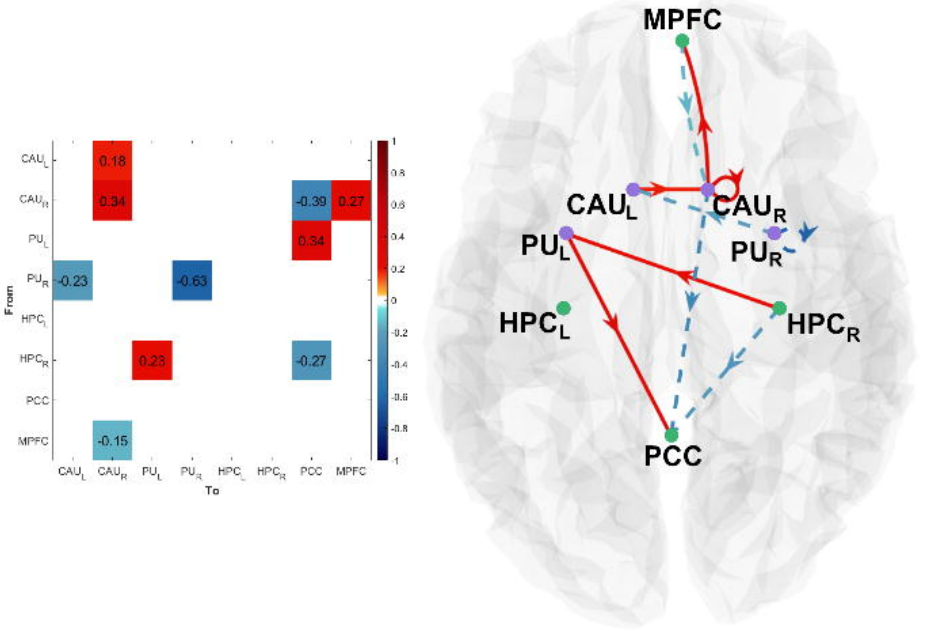

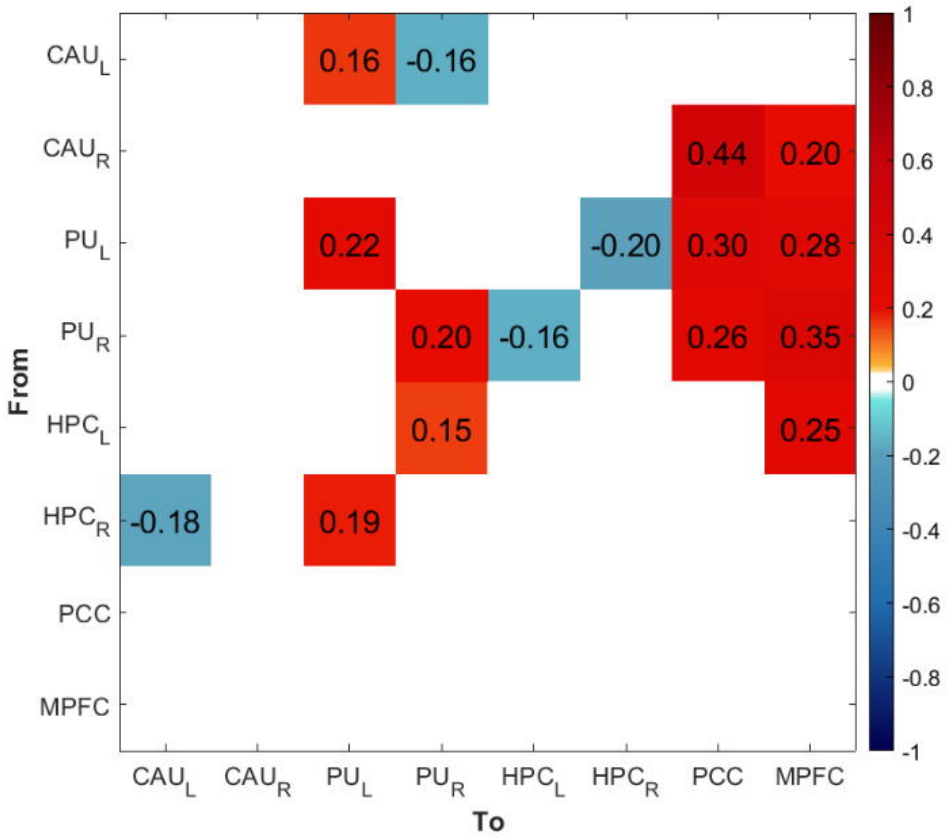
From
To
CAU_L
CAU_R
PU_L
PU_R
HPC_L
HPC_R
PCC
MPFC
0.16
-0.16
0.44
0.20
0.22
-0.20
0.30
0.28
0.20
-0.16
0.26
0.35
0.15
0.25
-0.18
0.19
1
0.8
0.6
0.4
0.2
0
-0.2
-0.4
-0.6
-0.8
-1

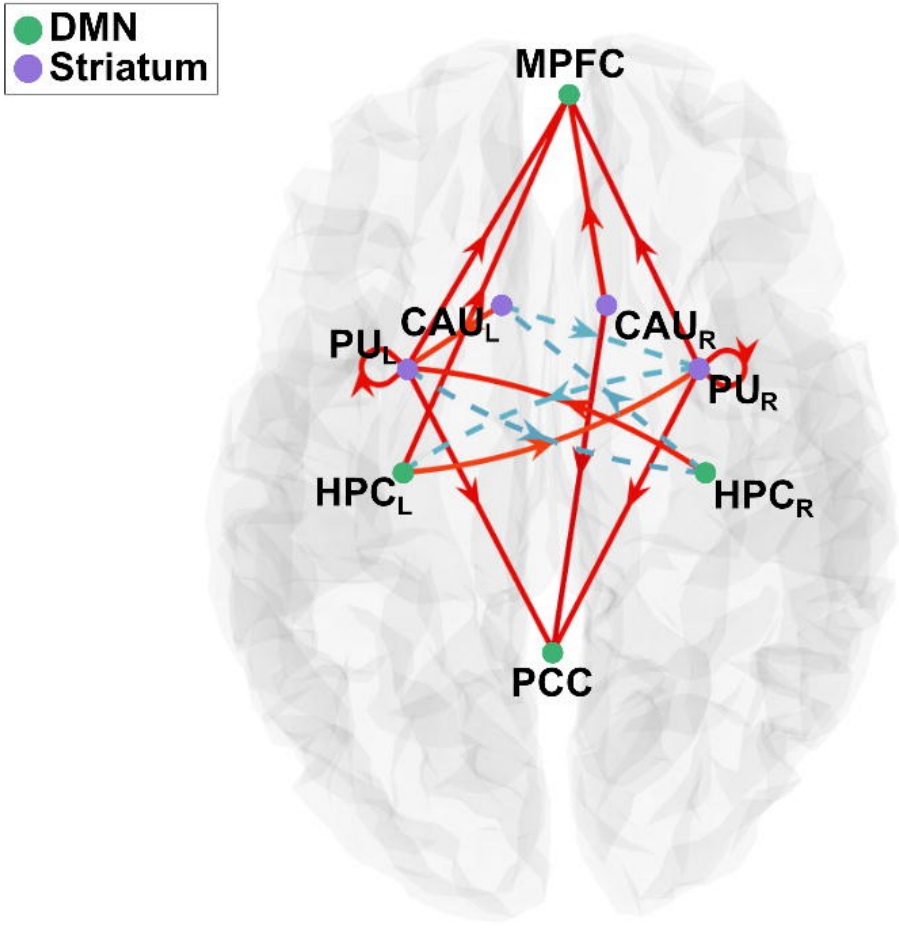
DMN
Striatum
MPFC
CAU_L
CAU_R
PU_L
PU_R
HPC_L
HPC_R
PCC

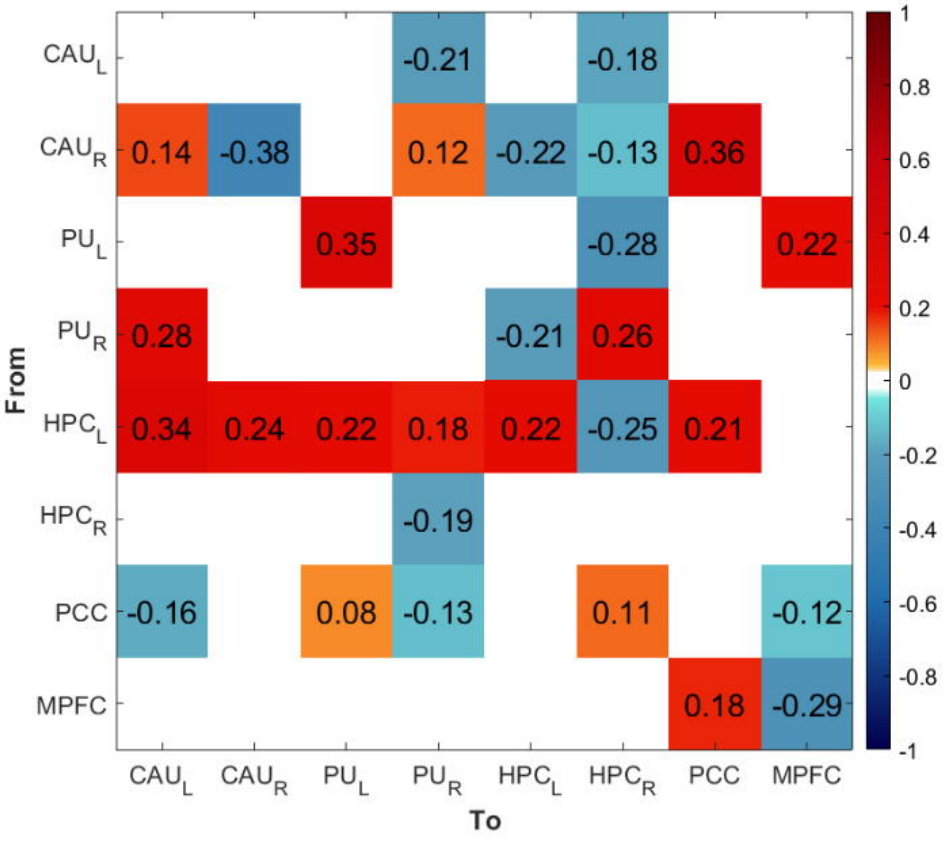
From
To
CAU_L
CAU_R
PU_L
PU_R
HPC_L
HPC_R
PCC
MPFC
-0.21
-0.18
0.14
-0.38
0.12
-0.22
-0.13
0.36
0.35
-0.28
0.22
0.28
-0.21
0.26
0.34
0.24
0.22
0.18
0.22
-0.25
0.21
-0.19
-0.16
0.08
-0.13
0.11
-0.12
0.18
-0.29
1
0.8
0.6
0.4
0.2
0
-0.2
-0.4
-0.6
-0.8
-1

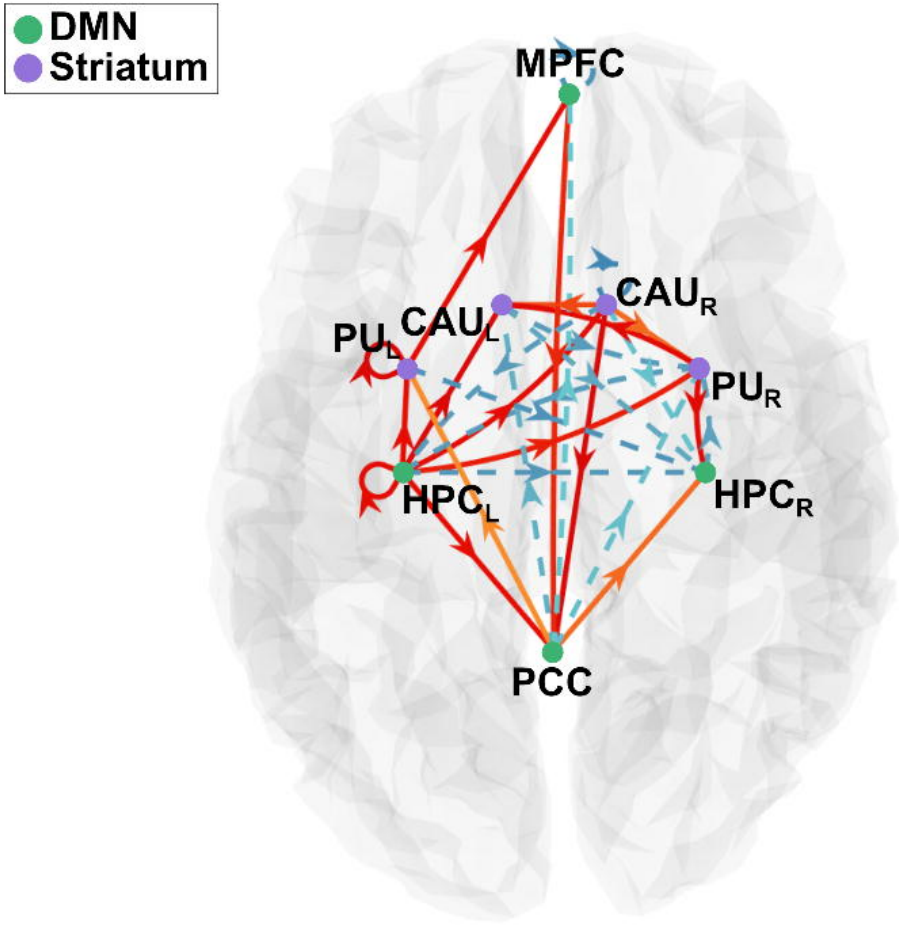
DMN
Striatum
MPFC
CAU_R
PU_L
CAU_L
PU_R
HPC_L
HPC_R
PCC

Table 1 Region of Interest Montreal Neurological Institute Coordinates

		Montreal Neurological Institute Coordinates			
Region of Interest	**Network**	**X**	**Z**	**Y**	**Size of Sphere**
MPFC	Default Mode Network	3	54	-2	8 mm
PCC	Default Mode Network	0	-52	26	8 mm
Left Hippocampus	Default Mode Network	-29	-18	-16	6 mm
Right Hippocampus	Default Mode Network	29	-18	-16	6 mm
Left Caudate	Striatum	-10	14	0	6 mm
Right Caudate	Striatum	10	14	0	6 mm
Left Putamen	Striatum	-28	2	0	6 mm
Right Putamen	Striatum	28	2	0	6 mm

MPFC = Medial Prefrontal Cortex; PCC = Posterior Cingulate Cortex.

Table 2 Demographic, Clinical, and Psychiatric Characteristics of Participant Groups

	History of Depression (N=30)	No History of Depression (N=68)	p value
Sex			0.059[a]
Female	19 (63.33%)	29 (42.65%)	
Male	11 (36.67%)	39 (57.35%)	
Age			0.824[b]
Mean (SD)	43.13 (6.68)	42.68 (10.32)	
Range	28.00 - 60.00	23.00 - 68.00	
Ethnicity			0.639[a]
American - Latin	1 (3.33%)	1 (1.47%)	
Asian - East	0 (0.00%)	2 (2.94%)	
Mixed	0 (0.00%)	1 (1.47%)	
White	29 (96.67%)	64 (94.12%)	
Handedness			0.089[a]
Ambidextrous	2 (6.67%)	2 (2.94%)	
Left-handed	4 (13.33%)	2 (2.94%)	
Right-handed	24 (80.00%)	64 (94.12%)	
HD-related Variables			
CAG Repeat Length			0.515[b]
Mean (SD)	43.10 (1.90)	43.43 (2.43)	
Range	39.00 - 47.00	40.00 - 49.00	
UHDRS TMS Score			0.887[b]
Mean (SD)	5.67 (4.74)	5.79 (3.74)	
Range	0.00 - 22.00	0.00 - 21.00	
CAP Score			0.860[b]
Mean (SD)	85.78 (10.89)	85.30 (13.01)	
Range	62.56 - 104.01	62.10 - 125.12	
DBS Score			0.912[b]
Mean (SD)	304.20 (59.12)	302.88 (51.89)	
Range	179.00 - 401.00	185.00 - 443.00	
Psychiatric Characteristics			
Current Depression			**< 0.001[a]**
No	12 (40.00%)	68 (100.00%)	
Yes	18 (60.00%)	0 (0.00%)	
BDI-II Score			0.064[b]
Mean (SD)	9.57 (11.32)	6.01 (7.19)	
Range	0.00 - 46.00	0.00 - 27.00	
BDI-II Cut-off			0.739[a]
Clinically elevated	8 (26.67%)	16 (23.53%)	
Not clinically elevated	22 (73.33%)	52 (76.47%)	
HADS-D Score			**0.020[b]**
Mean (SD)	4.73 (5.10)	2.62 (3.55)	
Range	0.00 - 19.00	0.00 - 14.00	
HADS-D Cut-off			0.213[a]

	History of Depression (N=30)	No History of Depression (N=68)	p value
Clinically elevated	7 (23.33%)	9 (13.24%)	
Not clinically elevated	23 (76.67%)	59 (86.76%)	
Current Mood Medication Use			**0.001**[a]
No	16 (53.33%)	57 (83.82%)	
Yes	14 (46.67%)	11 (16.18%)	
History of Suicidal Ideation			**0.041**[a]
No	19 (63.33%)	56 (82.35%)	
Yes	11 (36.67%)	12 (17.65%)	
History of Suicide Attempts			0.288[a]
No	27 (90.00%)	65 (95.59%)	
Yes	3 (10.00%)	3 (4.41%)	

Significant p values (≤ 0.05) are shown in bold. SD = standard deviation. CAG = cytosine-adenine-guanine. CAP = CAG-Age Product. DBS = Disease Burden Score. BDI-II = the Beck Depression Inventory, 2nd Edition. HADS-D = the Hospital Anxiety and Depression Scale, Depression Subscale.
[a]Pearson's Chi-squared test
[b]Linear Model ANOVA